

Reports

Point Mugu, California, Earthquake of 21 February 1973 and Its Aftershocks

Abstract. *Seismological investigations show that the Point Mugu earthquake involved north-south crustal shortening deep within the complex fault zone that marks the southern front of the Transverse Ranges province. This earthquake sequence results from the same stress system responsible for the deformation in this province in the Pliocene through Holocene and draws attention to the significant earthquake hazard that the southern frontal fault system poses to the Los Angeles metropolitan area.*

On 21 February 1973 a moderate-sized earthquake (magnitude $M_L = 6.0$) occurred in the vicinity of Point Mugu, California, causing minor damage to structures in the Oxnard region with no loss of life. No tectonic ground rupture was observed, and, except for anomalously large earth tilts that occurred at the time of the main shock along the Raymond Hill fault in Pasadena about 90 km east of the epicenter, surface effects can be attributed to seismic shaking. The earthquake occurred within a west-trending zone of deformation that marks the southern front of the Transverse Ranges province along the south flank of the Santa Monica Mountains. This zone, which can be traced eastward through Santa Monica, Hollywood, Los Angeles, Glendale, Pasadena, Monrovia, Glendora, and as far as Cajon Pass, north of San Bernardino, has undergone north-south crustal shortening by reverse faulting on north-dipping surfaces since at least Pleistocene time (1) possibly accompanied by left-lateral strike slip. The focal mechanism

of the main shock and the spatial distribution of the aftershocks are consistent with this mode of deformation; thus, it is probable that the stresses that caused the Pleistocene and Holocene deformation continue to the present.

The hypocentral coordinates of the main shock, determined with data from

regional seismograph stations (Fig. 1), are $34^{\circ}04.2'N$, $119^{\circ}02.0'W$ and a depth of 17 km. The uncertainty in the focal coordinates is estimated to be less than 5 km. The mode of faulting inferred from the P-wave fault plane solution for the main shock (Fig. 1) is north-over-south reverse slip accompanied by a smaller component of left-lateral strike slip on a plane that strikes $N69^{\circ}E$ and dips $49^{\circ}N$. The local magnitude, based on readings from four southern California stations, is $M_L = 6.0$. A body-wave magnitude of $m_b = 5.7$ and a surface-wave magnitude of $M_S = 5.2$ were reported for the main shock by the National Oceanic and Atmospheric Administration (2). This is the largest shock to occur along the southern frontal fault system of the Transverse Ranges province since at least 1932, when a network of seismic stations was established in southern California which made it possible to locate the events to within a few kilometers. The maximum horizontal acceleration recorded from the main shock was 0.13g, at a hypocentral distance of 25 km at Port Hueneme (Fig. 1). This value lies within the range of values observed at equivalent distances

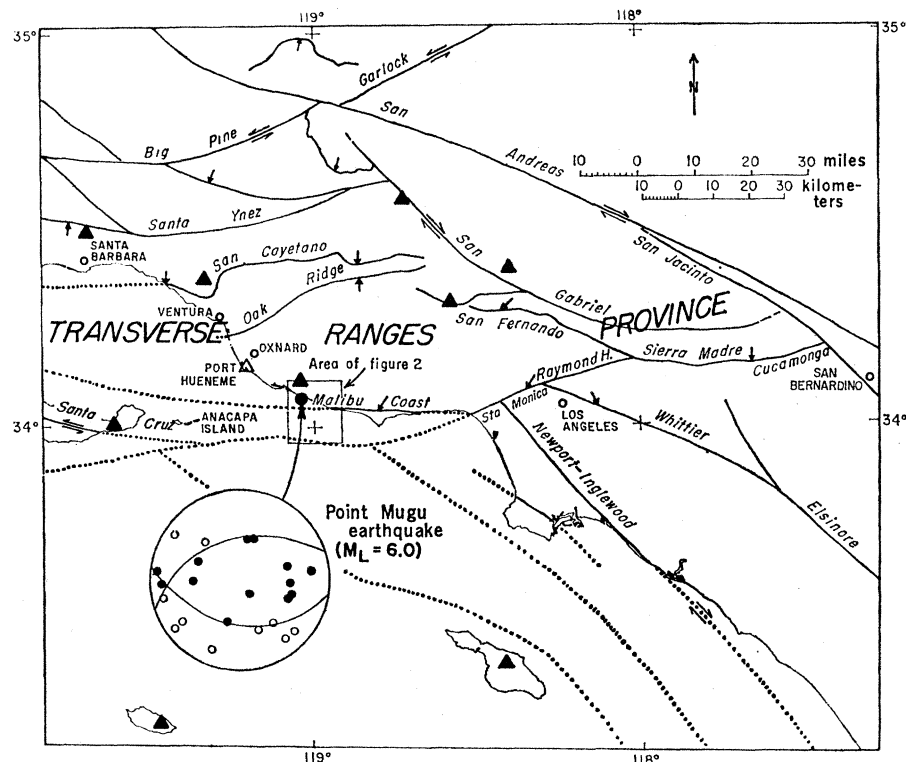


Fig. 1. Location and focal mechanism of the Point Mugu earthquake relative to the major fault systems. Double arrows on faults indicate the sense of strike slip motion. Single arrows on the upper block of thrust faults are inclined in the direction of known or suspected lateral displacement. The focal mechanism is represented by the equal-area, lower-hemisphere projection of P-wave first motions; closed circles denote compression, open circles dilatation. Closed triangles represent regional seismograph stations providing data for the location of the main shock. The open triangle is the strong-motion accelerograph site nearest the epicenter.

Scoreboard for Reports: In the past few weeks the editors have received an average of 68 Reports per week and have accepted 12 (17 percent). We plan to accept about 12 reports per week for the next several weeks. In the selection of papers to be published we must deal with several factors: the number of good papers submitted, the number of accepted papers that have not yet been published, the balance of subjects, and length of individual papers.

Authors of Reports published in *Science* find that their results receive good attention from an interdisciplinary audience. Most contributors send us excellent papers that meet high scientific standards. We seek to publish papers on a wide range of subjects, but financial limitations restrict the number of Reports published to about 15 per week. Certain fields are overrepresented. In order to achieve better balance of content, the acceptance rate of items dealing with physical science will be greater than average.

for other earthquakes of comparable magnitude (3).

Recent advances in seismic source theory (4) provide a basis for a more physical description of earthquakes than can be given by a single number such as magnitude. Source parameters for the main shock are estimated by two independent methods from low-gain ($\times 4$) torsion seismograms recorded at Pasadena (5). The first involves construction of synthetic seismograms produced by a propagating dislocation for various sets of source parameters. Synthetic seismograms (6) computed for a square dislocation surface on the fault plane dipping 49° toward $N21^\circ W$ and having equal left-lateral and reverse slip fit the observed seismograms reasonably well. If a bilateral rupture is assumed, the parameters are as follows: fault size, $5 \times 5 \text{ km}^2$; average fault slip, 15 cm; moment (M_0), 1.1×10^{24} dyne-cm; stress drop ($\Delta\sigma$), 11 bars; rise time of displacement dislocation, 0.5 second; and dislocation velocity, 30 cm/sec. If a unilateral rupture from west to east is assumed, the corresponding fault parameters are as follows: $2.5 \times 2.5 \text{ km}^2$, 30 cm, 0.6×10^{24} dyne-cm, 40 bars, 0.5 second, and 60 cm/sec, respectively. The second method involves estimation of the source parameters directly from the amplitude spectra of the seismograms, corrected for instrument response (7). The amplitude spectrum provides estimates of M_0 and the radius (r) of an equivalent circular source area. The average slip and $\Delta\sigma$ can in turn be derived from these parameters. With this method, M_0 is estimated to be 1.2×10^{24} dyne-cm, which is in good agreement with the values estimated from the propagating dislocation model. The source dimension is estimated to be $r = 1.6 \text{ km}$, resulting in an area slightly larger than the lower estimate inferred from the dislocation model. The three estimates of rupture area are smaller than the aftershock zone (40 to 50 km^2). The stress drop inferred from the spectral observations is 128 bars, considerably greater than the 11 to 40 bars estimated from the dislocation model; however, stress-drop estimates are typically subject to an uncertainty of a factor of 5. Relative to a large number of southern California earthquakes with source parameters similarly determined from amplitude spectra (7), the Point Mugu earthquake is a high stress-drop earthquake.

Quasi-static tilts associated with the

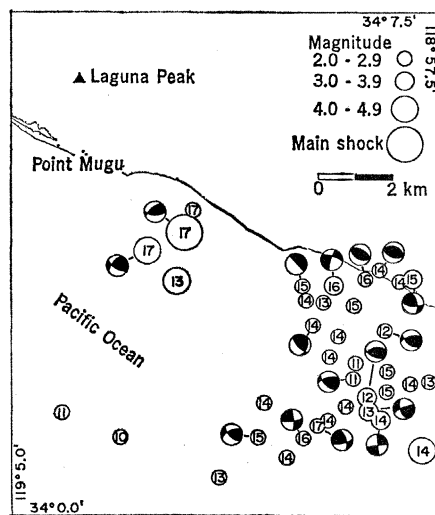


Fig. 2. Epicenters, focal depths (in kilometers), and reliable focal mechanism solutions of the main shock and larger aftershocks. Shaded regions of the lower-hemisphere focal mechanism diagrams are areas of compression, open regions are areas of dilatation.

Point Mugu earthquake were recorded at four tiltmeter stations along or adjacent to the Raymond Hill fault some 80 to 90 km east of Point Mugu. The observed tilts were several orders of magnitude greater than the tilt values that would be predicted from the main shock source parameters. It is possible to explain the observed tilts on the basis of a small dislocation on the Raymond Hill fault "triggered" by the passage of elastic waves from the Point Mugu earthquake through a prestressed area on the fault surface (8). Such a phenomenon was suggested (9) to explain the possible sympathetic fault slip associated with the 1968 Borrego Mountain earthquake.

Locations for the larger aftershocks and reliable focal mechanism solutions from the first week of the sequence (Fig. 2) reveal a complex pattern of strain release. The hypocenters of this sequence of earthquakes were unusually deep (10 to 17 km) by comparison with previously studied sequences in southern California. The attitude of the primary rupture surface is poorly defined by the aftershock hypocenters because the size of the aftershock zone is small relative to the estimated location uncertainties of 1 to 2 km in epicenter and 2 to 3 km in depth (10). Some aftershocks have focal mechanisms corresponding to north-south thrusting similar to the main shock; they occur about 6 km east to south-east of the main shock and about 2 to 4 km shallower. These events, together

with the main shock, possibly outline the perimeter of the primary rupture surface in the form of a triangular surface dipping roughly 30° northward. Focal mechanisms on the eastern edge of the aftershock zone reflect variations in the type of faulting ranging from nearly pure strike slip to nearly pure reverse slip. The orientation of the maximum compressional axis, however, is relatively stationary about a line east of north lying in a horizontal plane and is rotated about 45° clockwise from the axis for the main shock. The absence of aftershocks within the central part of the aftershock zone and the concentration of aftershocks along the eastern edge of the zone (Fig. 2) suggest that the rupture in the main shock effectively reduced the stresses in the central region and concentrated stress along the eastern perimeter of the rupture surface.

This earthquake sequence cannot be identified with any specific fault projected from onshore geologic mapping or inferred from acoustic profiles offshore, but it is clearly associated with the zone of deformation that marks the southern front of the Transverse Ranges province. The shocks center at depths well below the north-dipping Malibu Coast fault, in closer proximity to a steep north-dipping plane projected downward from the inferred seaward extension of the Santa Monica fault (Fig. 1). The diversity of focal mechanisms and the complex spatial distribution of hypocenters suggest that slip associated with the aftershocks was not confined to the primary rupture surface. This conclusion is compatible with the general style of Late Pleistocene and younger faulting in the rocks to the south of the Malibu Coast fault (11). Late Pleistocene marine and younger nonmarine terrace deposits have been displaced on several discontinuous, west-trending fault segments on which the dominant movement has been north-over-south reverse slip, probably with some associated left-lateral slip.

This earthquake sequence is similar to the San Fernando sequence of 9 February 1971 (12) in that both involved north-over-south reverse slip and left-lateral strike slip deformation along east-west fault zones that are characteristic of the Transverse Ranges province. The two earthquake sequences are also similar in the degree and character of the complexities associated with the spatial distribution

and focal mechanisms of the aftershocks. They differ, however, in the level and extent of aftershock activity which, in the San Fernando earthquake, was at least an order of magnitude greater and was distributed through an aftershock area that was larger by a factor of 20.

A second moderate-sized earthquake ($M_L=4.8$) occurred more recently within the southern frontal fault system of the Transverse Ranges province on 6 August 1973. This event, like the Point Mugu earthquake, was felt in southern California from Santa Barbara to the Los Angeles metropolitan area and beyond. The hypocenter was located 40 km west of Point Mugu and 7 km southwest of Anacapa Island, at a focal depth of 15 km. The P-wave focal mechanism solution, which is compatible with the sense of late Quaternary displacement on the Santa Cruz Island fault (13), is left-lateral strike slip movement along a fault plane striking east-west and dipping 70°S. This earthquake may have been associated with the eastern extension of that fault.

The Point Mugu and Anacapa Island earthquakes, like the San Fernando earthquake, focus attention on the likelihood that faults within the Transverse Ranges province on which movement occurred during Pleistocene time are seismically active today, and on the fact that serious seismic hazards are associated with the east-west fault systems transverse to the more widely publicized San Andreas fault system. Although the southern frontal fault system, comprised of the Malibu Coast, Santa Monica, Raymond Hill, Sierra Madre, and Cucamonga faults (Fig. 1), may not be capable of generating as large an earthquake as the San Andreas system, the frontal fault system passes directly through the Los Angeles metropolitan area and for this reason must be regarded as potentially as dangerous to the metropolitan area as the more distant San Andreas system.

W. L. ELLSWORTH, R. H. CAMPBELL
D. P. HILL, R. A. PAGE
National Center for Earthquake
Research, U.S. Geological Survey,
Menlo Park, California 94025
R. W. ALEWINE, III, T. C. HANKS
T. H. HEATON, J. A. HILEMAN
H. KANAMORI, B. MINSTER
J. H. WHITCOMB
Seismological Laboratory,
California Institute of Technology,
Pasadena 91109

14 DECEMBER 1973

References and Notes

1. W. F. Barbat, in *Habitat of Oil*, L. G. Weeks, Ed. (American Association of Petroleum Geologists, Tulsa, Okla., 1958), p. 62; R. H. Campbell and R. F. Yerkes, *Geol. Soc. Amer. Abstr. Program* (Cordilleran Section Meeting, 67th Annual Meeting) 3 (No. 2), 92 (1971).
2. *Natl. Oceanic Atmos. Admin. Earthquake Data Rep. 15-73* (1973), p. 16.
3. R. A. Page, D. M. Boore, W. B. Joyner, H. W. Coulter, *U.S. Geol. Surv. Circ. 672* (1972).
4. N. A. Haskell, *Bull. Seismol. Soc. Amer.* 54, 1181 (1964); *ibid.* 59, 865 (1969); K. Aki, *J. Geophys. Res.* 72, 1217 (1967); J. N. Brune, *ibid.* 75, 4997 (1970); J. C. Savage, *ibid.* 77, 3788 (1972).
5. An earthquake can be described by a dislocation model with the following parameters: A , the fault area; u , the average dislocation; and $\Delta\sigma$, the change in shear stress on the fault due to the introduction of the dislocation. The seismic moment is defined as $M_0 = \mu Au$, where μ is the rigidity of the medium. Relations between the other parameters can be derived for a particular dislocation model.
6. H. Kanamori, *Eos Trans. Amer. Geophys. Union* 54, 372 (1973).
7. W. R. Thatcher and T. C. Hanks, *J. Geophys. Res.*, in press.
8. T. H. Heaton and R. W. Alewine, III, *Stanford Univ. Publ. Univ. Ser. Geol. Sci.* 13, 94 (1973).
9. C. R. Allen, M. Wyss, J. N. Brune, A. Grantz, R. E. Wallace, *U.S. Geol. Surv. Prof. Pap.* 787 (1972), p. 87.
10. The pattern of first arrival times recorded on the temporary seismograph network installed along the coast adjacent to the epicentral area by the California Institute of Technology and the U.S. Geological Survey and on sonobuoys dropped in the epicentral region by the University of California, San Diego, reported by H. Bradner and J. N. Brune [*Seismol. Soc. Amer. 68th Annu. Nat. Meet. Program Abstr.* (1973), p. 7] indicates that the suite of hypocenters may lie 2 to 5 km north of the reported location and at a focal depth 1 to 2 km shallower. The relative location of the main shock hypocenter near the northwestern edge of the aftershock zone is confirmed by the similar pattern of first arrivals at regional stations for the main shock and for a nearby aftershock, recorded on both regional and local seismographs.
11. R. H. Campbell, B. A. Blackerby, R. F. Yerkes, J. E. Schoellhamer, P. W. Birkeland, C. M. Wentworth, "Preliminary geologic map of the Point Dume quadrangle, Los Angeles County, California" [U.S. Geological Survey Open-File Map (1970)]; R. F. Yerkes and C. M. Wentworth, "Structure, quaternary history, and general geology of the Corral Canyon area, Los Angeles County, California" [U.S. Geological Survey Open-File Report (1965)]; R. F. Yerkes, R. H. Campbell, B. A. Blackerby, C. M. Wentworth, P. W. Birkeland, J. E. Schoellhamer, "Preliminary geologic map of the Malibu Beach quadrangle, Los Angeles County, California" [U.S. Geological Survey Open-File Map (1971)].
12. U.S. Geological Survey, *U.S. Geol. Surv. Prof. Pap.* 733 (1971).
13. W. W. Rand, *Calif. J. Mines Geol.* 27, 214 (1931); C. S. J. Bremner, *Santa Barbara Mus. Nat. Hist. Occas. Pap.* 1 (1932).
14. Contribution No. 2382, Division of Geological and Planetary Sciences, California Institute of Technology. Publication authorized by the Director, U.S. Geological Survey.

30 August 1973

Premonitory Variations in S-Wave Velocity Anisotropy before Earthquakes in Nevada

Abstract. *Application of nonhydrostatic stress to rock induces velocity anisotropy, causing the S wave to split into two components traveling with somewhat different velocities. Large premonitory changes in the extent of S-wave splitting have been observed for two earthquakes in Nevada. Observations of the difference between the two S-wave velocities may provide a simple method for predicting earthquakes.*

Recent laboratory and theoretical studies have shown that the application of nonhydrostatic stress to rock containing cracks induces appreciable velocity anisotropy of S waves (1, 2). For an anisotropic medium, there are, in general, three velocities of elastic wave propagation and only in special directions do these reduce to purely compressional (P) and purely shear (S) motion. The S wave splits into two distinct components traveling with velocities that are generally different along a given direction of wave propagation.

This phenomenon has been called "acoustic double refraction" (1, 3) owing to its apparent similarity to the production of double refraction in glass by the application of stress. The separation between the two components of the S wave increases with increasing deviatoric stress. I describe here my observations of significant temporal changes in the extent of S-wave splitting

Table 1. Criteria for identifying SH, SV phases at Tonopah for events near Mina.

Phase SH	
1)	Little or no motion on the vertical instrument
2)	First motions generally west and south on the east-west and north-south instruments
3)	In-phase trace motions on the east-west and north-south instruments
Phase SV	
1)	First motions generally down, east, and south
2)	(a) Out-of-phase trace motions on the vertical and east-west instruments (b) In-phase trace motions on the vertical and north-south instruments
3)	Wave form of SV as seen on the vertical instrument similar to that of SH seen on the east-west or north-south instrument